Volume 120 Number 3 September 2000

The Journal of
THORACIC AND CARDIOVASCULAR SURGERY

GENERAL THORACIC SURGERY

LYMPHATIC DRAINAGE OF CARBON PARTICLES INJECTED INTO THE PLEURAL CAVITY OF THE MONKEY, AS STUDIED BY VIDEO-ASSISTED THORACOSCOPY AND ELECTRON MICROSCOPY

Takashi Miura, MD[a]
Tatsuo Shimada, MD[b]
Koichi Tanaka, MD[a]
Masao Chujo, MD[a]
Yuzo Uchida, MD[a]

Objectives: The aim of this study was to clarify the dynamics of lymphatic drainage of the pleural cavity to understand the mechanism of malignant pleural effusion.

Methods: We injected carbon particles into the pleural cavity of monkeys subjected to *general* anesthesia. We then observed the parietal pleura with a video-assisted thoracoscope and scanning and transmission electron microscopes to examine the regions of the parietal pleura where the carbon particles had been absorbed.

Results: The video-assisted thoracoscope showed that the carbon particles had gone directly to the costal, mediastinal, and diaphragmatic pleura by 10 to 15 minutes after injection. From the scanning and transmission electron microscopes, we found that the parietal pleura in the costal and mediastinal regions consisted of 3 elements: a layer of small mesothelial cells, the macula cribriformis, and lymphatic lacunae. Stomata (3-5 μm in diameter) were found between the small mesothelial cells. The macula cribriformis was composed of densely packed collagen fibrils and had many foramina (3-10 μm in diameter). Intrapleurally injected carbon particles were carried into the lymphatic lacunae via the stomata and vesicles of the mesothelial cells

From the Departments of Surgery II[a] and Fundamental Nursing,[b] Oita Medical University, Oita, Japan.

Received for publication Dec 7, 1999; revisions requested April 18, 2000; revisions received May 12, 2000; accepted for publication May 12, 2000.

Address for reprints: Takashi Miura, MD, Department of Surgery II, Oita Medical University, Hasama-machi, Oita, 879-5593, Japan (E-mail: tmiu@oita-med.ac.jp).

J Thorac Cardiovasc Surg 2000;120:437-47

0022-5223/2000 $12.00 + 0 **12/1/108906**

doi:10.1067/mtc.2000.108906

The Journal of Thoracic and
Cardiovascular Surgery
September 2000

and the foramina of the macula cribriformis. The lymphatic lacunae filled with carbon particles were richly distributed in both the anterior costal pleura and the mediastinal pleura.

Conclusion: We suggest that the mesothelial stomata and the macula cribriformis are structures essential to the absorption of macromolecules and cellular elements from the pleural cavity into the lymphatic system. (J Thorac Cardiovasc Surg 2000;120:437-47)

The prognosis of patients with lung cancer who have malignant pleural effusion is thought to be generally poor. For this type of effusion to be understood better, it would be valuable to define the structure and distribution of the lymphatic system in the parietal pleura. Intrapleurally injected particulate matter[1] and erythrocytes[2] are known to drain mainly to the parietal pleura. Studies with a scanning (SEM) and transmission electron microscope (TEM) have illustrated that the parietal pleura of the rat[3] and sheep[4] consists of a single layer of mesothelial cells and that stomata are interposed between the mesothelial cells. These stomata connect the pleural cavity and the submesothelial lymphatic capillaries.[5] Recently, an enzyme histochemical technique used to identify lymphatic vessels[6,7] demonstrated that the lymphatics in the costal pleura of the monkey ran parallel to the intercostal muscle fibers and that, in the mediastinal pleura, these lymphatics had a treelike appearance.[8] Particulate matter injected into the pleural cavity probably drains into the lymphatic capillaries via the pleural stomata. However, this remained to be clarified.

Using a silver-impregnation technique capable of demonstrating collagen and reticular fibers, Kihara[9,10] and Tubouti[11,12] detected a sievelike structure in the submesothelial connective tissue of the human diaphragm and costal pleura. This characteristic structure was named the *macula cribriformis,* and the researchers suggested that it formed a prelymphatic fluid pathway in the submesothelial connective tissue. In addition, they suggested that the macula cribriformis was closely involved with tumor infiltration into the diaphragm.[13] Recently, the sodium hydroxide (NaOH) maceration–SEM method was used to demonstrate that the macula cribriformis in the diaphragm was located between the peritoneal mesothelial cells with stomata and the subperitoneal lymphatic capillaries.[14,15]

The first aim of our study was to examine the presence and 3-dimensional structure of the macula cribriformis in the parietal pleura of the monkey by SEM and to elucidate the topographic relationship between the macula cribriformis and mesothelial stomata or subpleural lymphatic lacunae. The second aim was to clarify the kinetics of lymphatic drainage in the parietal pleura. These aims were fulfilled by using video-assisted thoracoscopy, TEM, and SEM to examine the absorption of carbon particulates (CH40) injected into the pleural cavity of the monkey during normal breathing.

Materials and methods

Stereoscopic and electron microscopic studies. Three Japanese monkeys *(Macaca fuscata)* weighing 8 to 12 kg were used. The animals were fed in accordance with our university's guidelines for the care of experimental animals. They were deeply anesthetized with an intramuscular injection of ketamine hydrochloride (5 mg/kg), followed by an intraperitoneal injection of sodium phenobarbital (25 mg/kg). They were placed in a lateral recumbent position with orotracheal intubation. After 2 mL of carbon particles[16] (Nacalai Tesque, Inc, Kyoto, Japan) had been injected diffusely into the pleural cavity, the lung was reinflated by continuous suction. After 90 minutes of spontaneous respiration, the animals were put to death by exsanguination and perfused with a fixative of 2.5% glutaraldehyde and 2% paraformaldehyde in cacodylate buffer (0.1 mol/L), pH 7.4 (Karnovsky fixative) given through the abdominal aorta and infused into the pleural cavity. After the pleural cavity had been washed out with saline solution, the parietal pleura was examined with a stereoscope, and the lymphatic system was photographed. For the SEM study the tissues were first examined macroscopically; then 1-cm^2 block samples of those areas of parietal pleura containing absorbed carbon particles were taken from the costal, mediastinal, and diaphragmatic regions. They were immersed in the Karnovsky fixative for 2 hours. Some of the tissue blocks were washed thoroughly with saline solution. Others were immersed in 2N NaOH at 37°C for 2 hours to expose the submesothelial connective tissue. These blocks were postfixed in cacodylate-buffered (pH 7.4) 1% osmium tetroxide for 2 hours and dehydrated in a graded series of ethanol, dried by the *t*-butyl alcohol drying method, sputter coated, and viewed

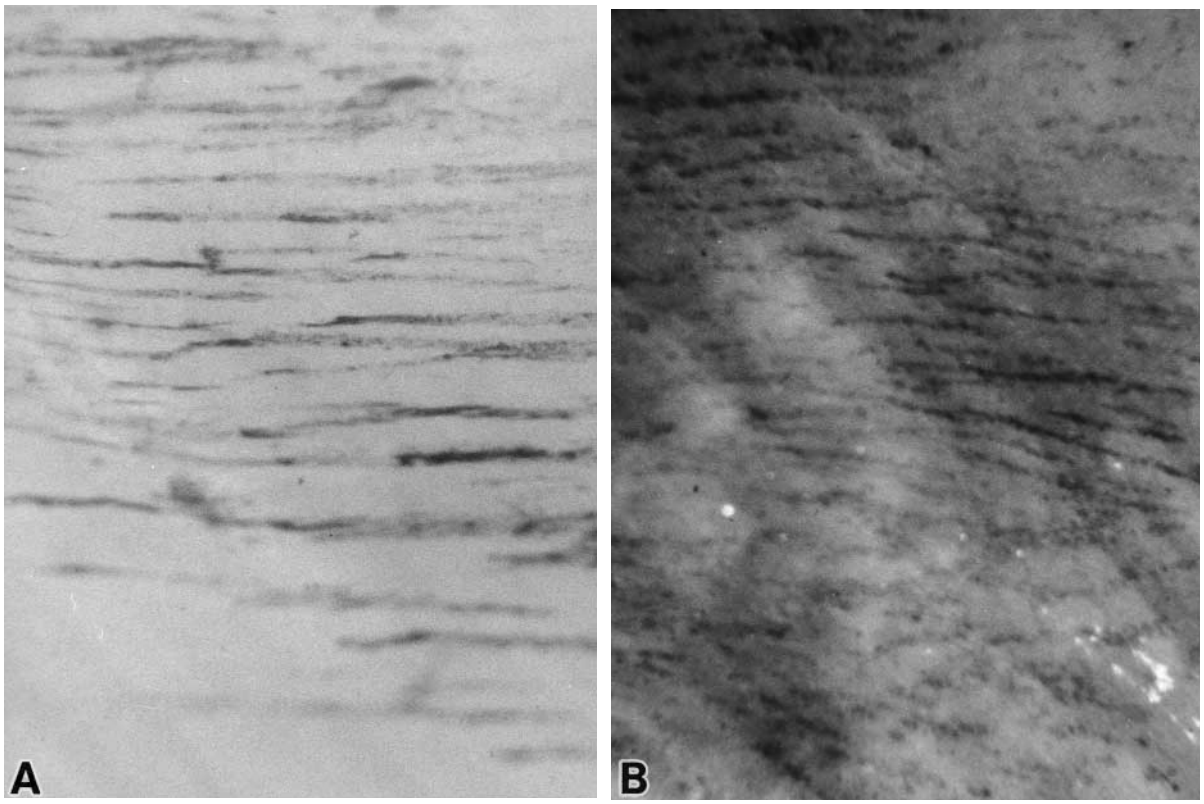

Fig 1. Steroscopic images showing that intrapleurally injected carbon particles enter the network of the subpleural lymphatic lacunae. The lymphatic lacunae in the costal pleura run parallel to the rib **(A),** and those in the mediastinal pleura are dense in the region surrounding the aortic hiatus **(B).** (Original magnification × 30.)

under an H-800 SEM (Hitachi, Ltd, Tokyo, Japan). For TEM, the parietal pleura was cut into small pieces, immersed in the Karnovsky fixative for 2 hours, and postfixed in cacodylate-buffered (pH 7.4) 2% osmium tetroxide/1% potassium ferrocyanide for 2 hours. They were then dehydrated in a graded series of ethanol and embedded in epoxy resin. Thin sections were cut, stained with methanolic uranyl acetate and aqueous lead citrate, and viewed under a JEOL-100CX TEM (JEOL Ltd, Akishima, Japan).

Video-assisted thoracoscopic study. We used 3 Japanese monkeys *(Macaca fuscata)* weighing 8 to 12 kg. The animals were deeply anesthetized by the technique mentioned above and placed in a lateral recumbent position with orotracheal intubation. A video-assisted thoracoscope (5 mm in diameter, 30°; Olympus Optical Co, Ltd, Tokyo, Japan) was then inserted into the pleural cavity through the seventh intercostal space. When the pleural cavity was opened the lung naturally collapsed as a result of the spontaneous breathing. After a 2-mL solution of carbon particles had been injected diffusely into the pleural cavity via the other port, the lung was reinflated by continuous suction. The pleural cavity and the lymphatic drainage of carbon particles in the parietal pleura were observed by video-assisted thoracoscopy every 10 to 15 minutes.

Results

Distribution of the lymphatic system in the parietal pleura. With the naked eye and the stereomicroscope, we confirmed that carbon particles injected into the pleural cavity had been taken up by the lymphatic lacunae and vessels of the parietal pleura by 1 hour after injection. The lymphatic capillaries (lacunae) filled with carbon particles were distributed in the superficial layer of the costal pleura and mediastinal pleura surrounding the esophageal hiatus and aortic hiatus. The lacunae in the costal pleura ran parallel to the intercostal muscle fibers (Fig 1, *A*), and those in the mediastinal pleura showed a reticular pattern (Fig 1, *B*). We found that the carbon particles were richly absorbed into the lymphatic lacunae in the costal pleura near the internal thoracic vessels. In addition, injected carbon particles were found in the parasternal and mediastinal trunks.

SEM study. We used SEM to examine the areas of the costal pleura that had absorbed the injected carbon particles. We recognized two structurally different types of mesothelial cells in the costal pleura. One

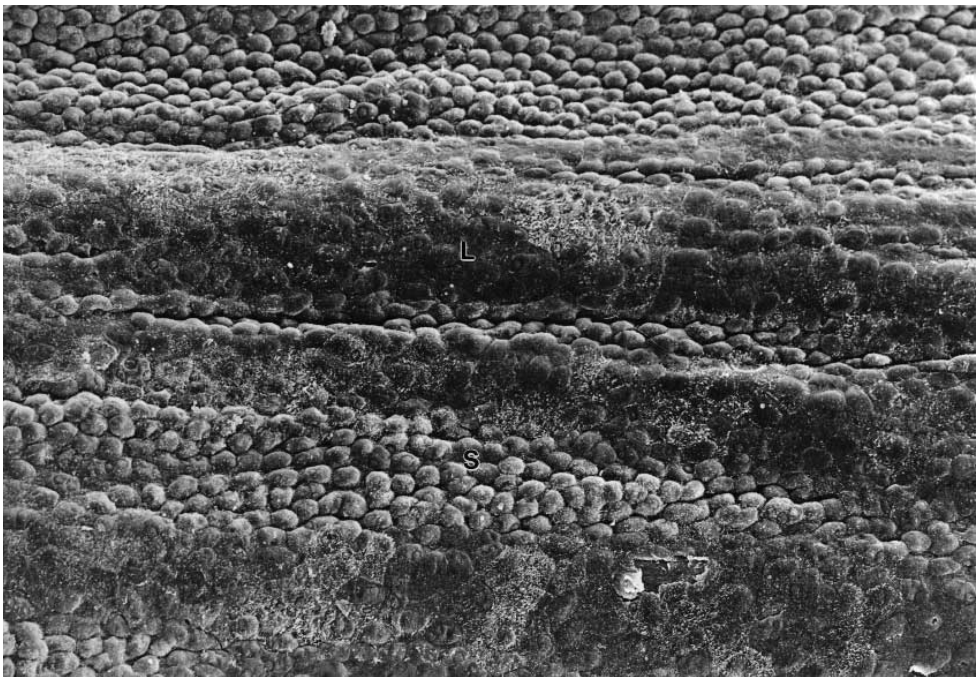

Fig 2. SEM of the inner surface of the monkey costal pleura. Areas consisting of smaller *(S)* cuboidal and larger *(L)* flat mesothelial cells can be recognized. The arrangement of small cell groups is similar to that of subpleural lymphatic lacunae. (Original magnification ×150.)

had a flattened shape and was approximately 15 to 20 μm in diameter. The other cell type was small, with rounded apices. These two types of cells formed groups that were arranged alternately (Fig 2). The apical surfaces of the smaller mesothelial cells had short microvilli and microprojections. We recognized small holes (stomata) 4 to 8 μm in diameter between these cells. The endothelial cells of the submesothelial lymphatic lacunae were visible through these stomata (Fig 3). In contrast, the larger mesothelial cells had numerous microvilli but no stomata. On the basis of these findings, it appears that the lymphatic lacunae were situated beneath the groups of smaller mesothelial cells with stomata. In the samples of costal pleura treated with 2N NaOH at 37°C for 30 minutes, some of the mesothelial cells had been removed and the submesothelial connective tissues had been exposed. Numerous foramina 3 to 8 μm in diameter, consisting of collagen fibers, were visible in the submesothelial connective tissues. These foramina were distributed just beneath the smaller mesothelial cell groups (Fig 4). The endothelial cells of the subpleural lymphatic lacunae were also visible through these foramina. The stomata between the smaller mesothelial cells were connected with the foramina. Furthermore, intrapleurally injected carbon particles were seen in the foramina. In the samples of costal pleura treated with 2N NaOH at 37°C for 1 to 2 hours, all the mesothelial cells had been removed by the maceration process, and the submesothelial connective tissues could be satisfactorily examined by SEM. The submesothelial connective tissues looked like a sheet and had a sieve-like structure. This peculiar structure with numerous foramina was fundamentally the same as that of the macula cribriformis demonstrated in the monkey diaphragm.[14,15] The macula cribriformis in the costal pleura ran parallel, and it was arranged in accordance with the arrangement of the smaller mesothelial cell group and the subpleural lymphatic lacunae. At high magnification, the macula cribriformis appeared to consist of dense collagen fibrils. In the areas without foramina, where the macula cribriformis was not present, there were very small spaces (approximately 1-2 μm) between the collagen fibrils (Fig 5). In conclusion, the SEM study of the parietal pleura revealed that the macula cribriformis was situated between the mesothelial cell groups with stomata and the submesothelial lymphatic lacunae.

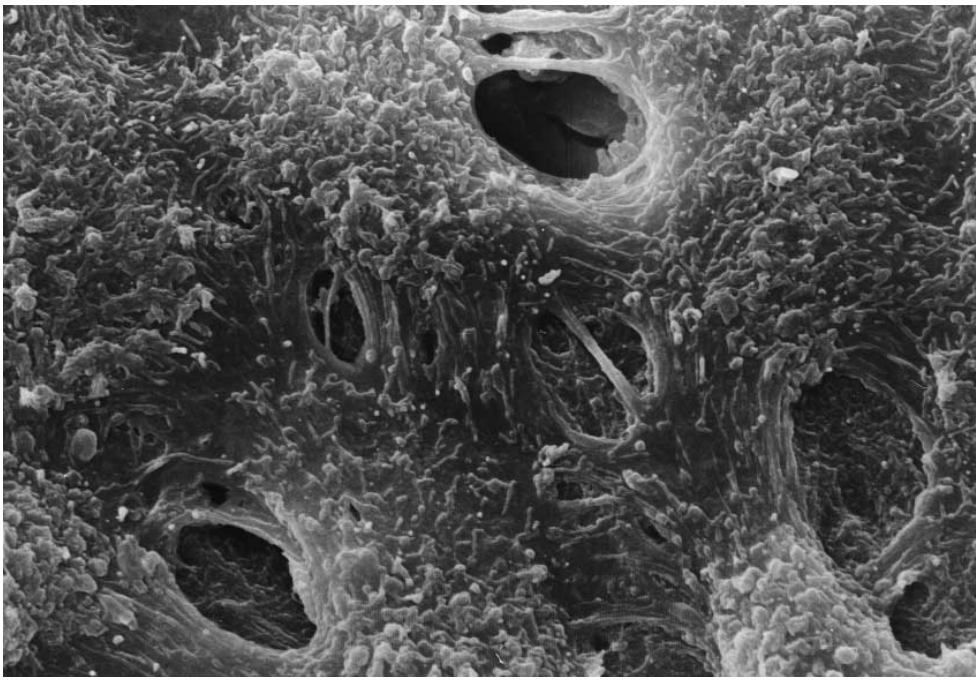

Fig. 3. SEM of stomata can be seen between smaller cuboidal mesothelial cells. The lymphatic endothelial cell can be seen through stomata. (Original magnification × 3300.)

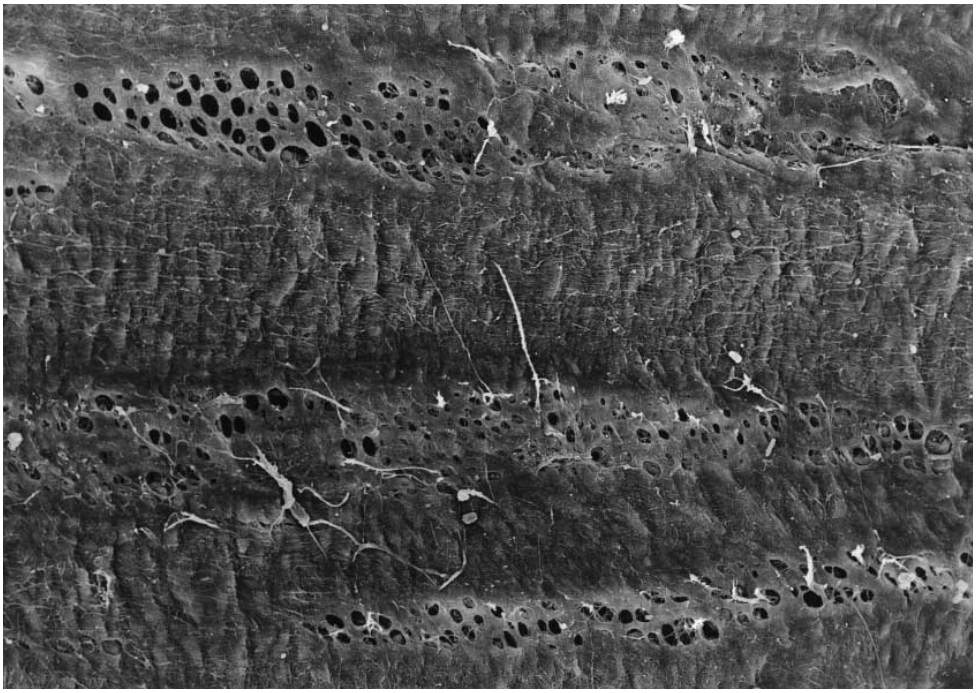

Fig. 4. SEM of the costal pleura treated with 2N NaOH for 4 hours at 37°C. The subpleural connective tissue layer is visualized by removal of mesothelial cells, showing a sievelike appearance. This structure corresponds to the macula cribriformis and possesses many foramina. (Original magnification × 280.)

The Journal of Thoracic and
Cardiovascular Surgery
September 2000

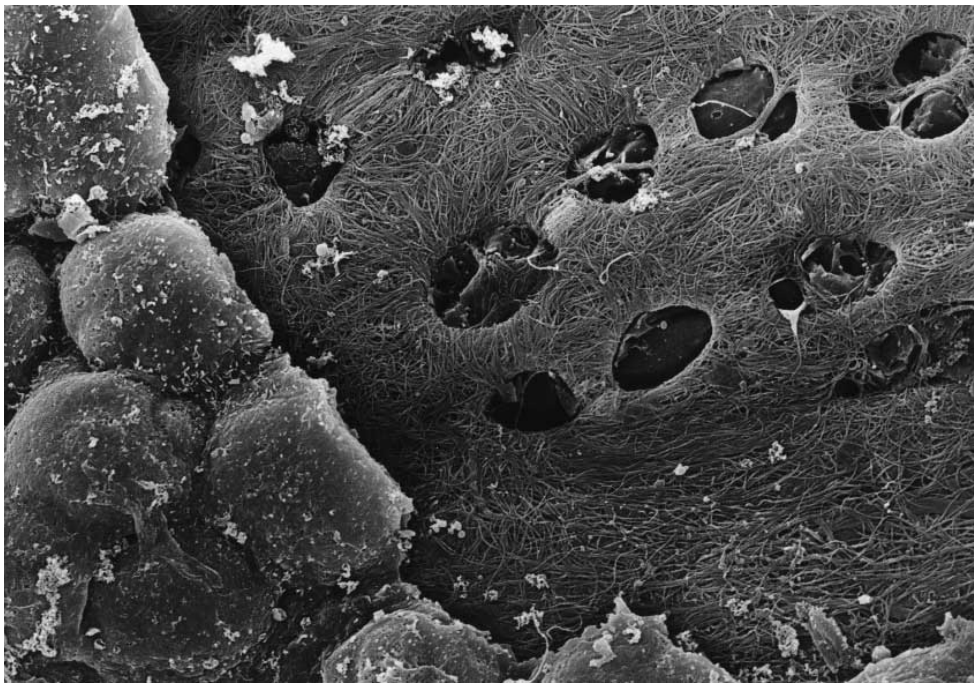

Fig 5. SEM of the costal pleura treated with 2N NaOH for 30 minutes at 37°C. Some of small mesothelial cells are partially removed, and the macula cribriformis with foramina are visible beneath them. The macula cribriformis consists of collagen fibrils, and the abluminal surface of the lymphatic endothelial cells can also be seen. (Original magnification × 1100.)

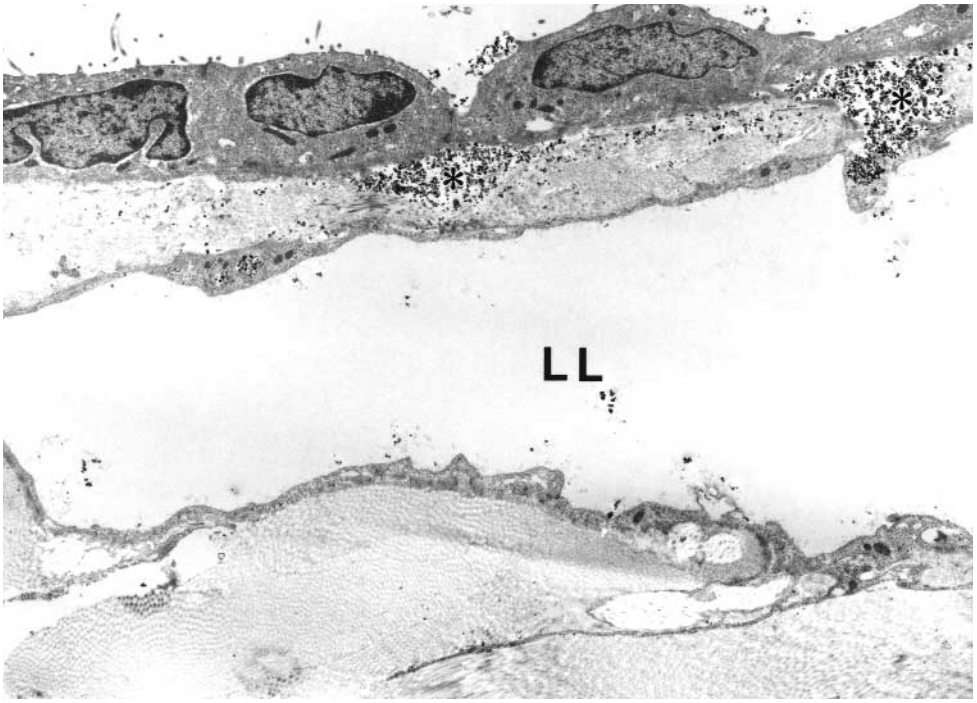

Fig 6. TEM of the costal region where intrapleurally injected carbon particles were absorbed. Carbon particles can be seen in the macula cribriformis *(asterisks)* beneath smaller mesothelial cells and in the lumen of the lymphatic lacuna *(LL).* (Original magnification × 2200.)

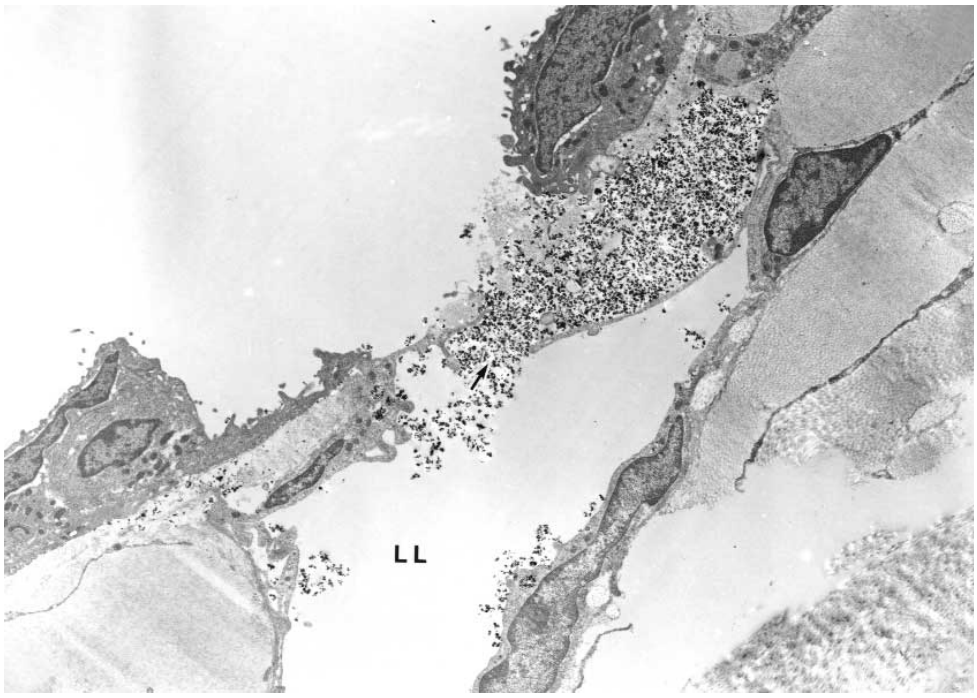

Fig 7. TEM showing that intrapleurally injected carbon particles pass through a stoma into the lumen of the lymphatic lacunae *(LL).* Note that carbon particles pass the intracellular space *(arrow)* of the lymphatic endothelial cells. (Original magnification × 2000.)

TEM study. We also clarified that the lymphatic lacunae were distributed beneath the mesothelial cells (Fig 6). Carbon particles injected into the pleural cavity were taken up by the lymphatic lacunae of the parietal pleura after 30 minutes. TEM analysis of the costal pleura revealed that carbon particles entered the lumina of the subpleural lymphatic lacunae mainly via the mesothelial stomata (Figs 7 and 8). Carbon particles were found in small vesicles and vacuoles in the cytoplasm of the smaller mesothelial cells (Fig 7), but few carbon particles were seen in the cytoplasm of the larger mesothelial cells. The numbers of carbon particles taken into the cytoplasm of the smaller mesothelial cells had increased by 60 minutes after injection. Our most interesting finding was that a great number of carbon particles were found in the large spaces in the submesothelial connective tissues, which were collagen bundles (Figs 6 to 8). These submesothelial spaces apparently corresponded to the foramina of the macula cribriformis. The carbon particles, carried from the pleural cavity into the foramina of the macula cribriformis, had to pass the walls of the lymphatic lacunae to enter their lumina. Carbon particles could be found in the spaces between neighboring lymphatic endothelial cells (Fig 8). Furthermore, they frequently appeared to stick to the vesicles and small vacuoles opening into the lymphatic lumina (Fig 7).

Video-assisted thoracoscopic study. We opened the pleural cavity 10 minutes after the intrapleural injection of carbon particles, and the lung collapsed naturally during spontaneous breathing. We were then able to examine the lymphatic drainage of carbon particles in the parietal pleura every 10 to 15 minutes through video-assisted thoracoscopy. We confirmed the presence of lymphatic drainage of injected carbon particles in the costal pleura near the intrathoracic vessels (Fig 9, *A*), the diaphragmatic pleura (Fig 9, *B*), and the mediastinal pleura containing the hilum of the lung, the aortic arch, the aortic hiatus, and the esophageal hiatus. Carbon particles had been absorbed into the lymphatics of the diaphragmatic pleura by 10 minutes after injection (Fig 10, *A*). By 30 minutes after injection, the carbon particles had disappeared from this area (Fig 10, *B*); most had been carried to the parasternal region (Fig 11).

Discussion

Since the pleura plays an important role in pulmonary function and in a variety of diseases, much attention has been paid to the details of its structure. Recent knowledge of pleural morphology is based on descriptions

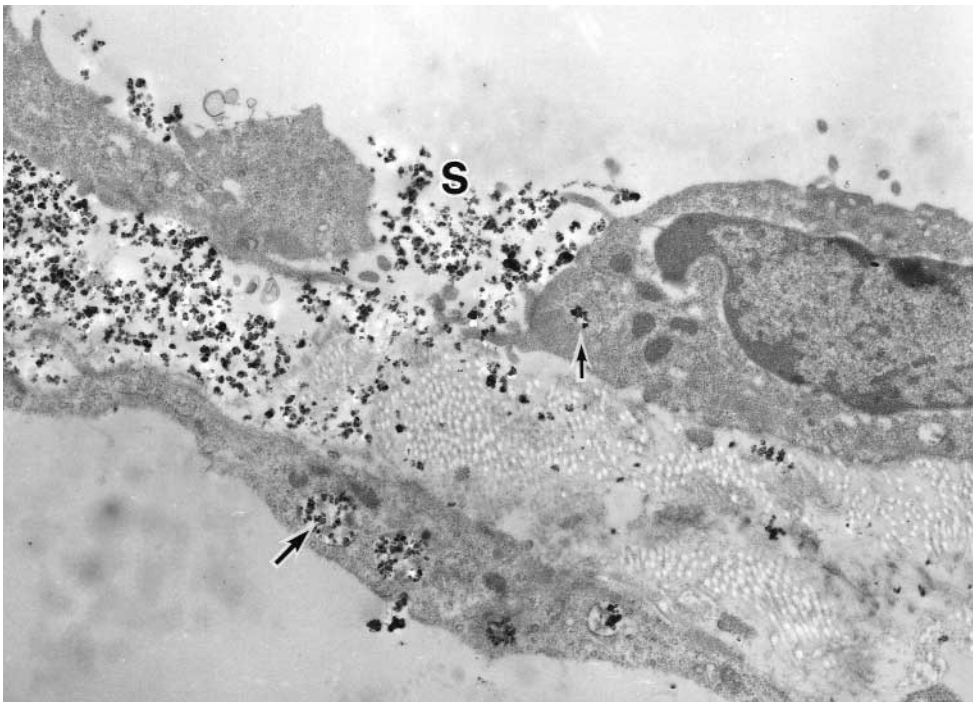

Fig 8. TEM of the costal pleura. There are carbon particles in vacuoles *(small arrow)* of the smaller mesothelial cell, the subpleural connective tissue space, and vacuoles *(large arrow)* of the lymphatic endothelial cell in addition to the stoma *(S)*. (Original magnification × 5000.)

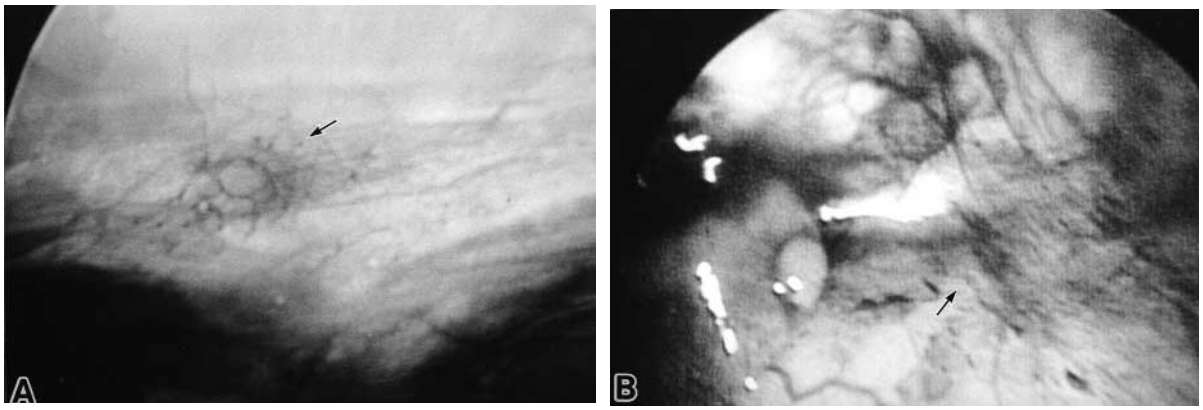

Fig 9. Video-assisted thoracoscopic images of the parietal pleura 10 minutes after intrapleural injection with carbon particles. Carbon particles are absorbed at the costal pleura near the intrathoracic vessels (*arrow;* **A**) and at the diaphragmatic pleura (*arrow;* **B**).

attained by light microscopy, SEM, and TEM. The parietal pleura is known to have openings (mesothelial stomata) connecting the pleural cavity with the submesothelial lymphatic system. The stomata are known to be distributed in the anterior costal pleura in human beings, rodents, rabbits, and sheep.[4,17-19] In the monkeys used in our study, the rich distribution of these stomata was recognized by SEM, both at the anterior costal pleura and at the mediastinal pleura. Although sparsely distributed stomata have been reported in the human diaphragmatic pleura,[20] we failed to detect stomata in the diaphragmatic pleura of the monkey. Further close

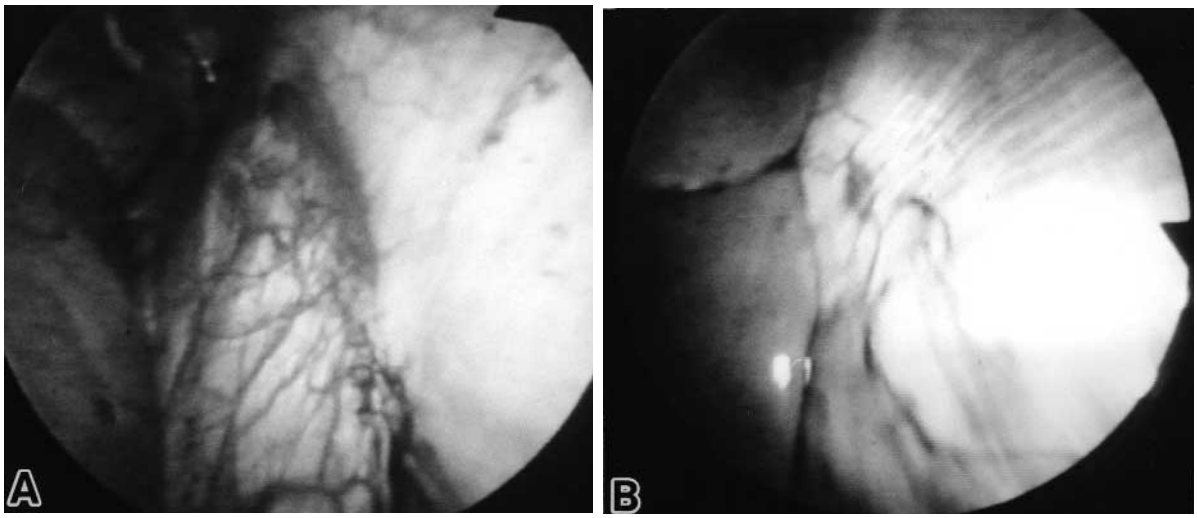

Fig 10. Video-assisted thoracoscopic images of the diaphragmatic pleura. Carbon particles can be seen in the subpleural lymphatics of the diaphragmatic pleura 10 minutes after injection **(A),** but they are nearly lost 30 minutes after injection **(B).**

observation may be needed. The monkey costal pleura, like that of the rat,[19] was covered with two different types of mesothelial cells: one small and round and the other large and flat. The stomata were present only between the former types of cells. The linear arrangement of the smaller cell groups was parallel to the intercostal muscle fibers, corresponding to the arrangement of the submesothelial lymphatics (lymphatic lacunae) that absorbed the injected carbon particles. Using a silver-impregnation technique capable of demonstrating collagen and reticular fibers, Kihara[9,10] and Tubouti[11,12] have detected a sievelike structure, the macula cribriformis, in the submesothelial connective tissue of the human diaphragm and parietal pleura. Recently, the existence of the macula cribriformis has been reported in the diaphragmatic pleura of the monkey, rat, and mouse in an SEM study that used a maceration technique.[14,15] Our SEM study demonstrated that the macula cribriformis was present between the mesothelial cells with stomata and the lymphatic lacunae. The size and number of foramina of the macula cribriformis were larger than those of the mesothelial stomata. The foramina of the macula cribriformis demonstrated by SEM appeared to correspond to those areas lacking collagen fibers, as demonstrated by TEM. From our SEM and TEM findings, we suggest that the foramina of the macula cribriformis also form short channels between the pleural cavity and the lymphatic lacunae or between the pleural mesothelial cells and the lymphatic lacunae. In some TEM studies of the costal pleura of rats and

Fig 11. Video-assisted thoracoscopic images of the anterior costal pleura. Carbon particles mainly drained to the parasternal portion 30 minutes after being injected intrapleurally *(arrow).*

rabbits intrapleurally injected with particulates, carbon particles or blood cells were found to reach the lumina of the lymphatic lacunae through mesothelial stomata and the interendothelial spaces of the lymphatic lacunae.[5,7,19] In our monkeys, intrapleurally injected carbon particles were found in the cytoplasmic vesicles and vacuoles of the mesothelial and lymphatic endothelial cells, as well as in the stomata and interendothelial spaces mentioned above. Massive carbon particles were

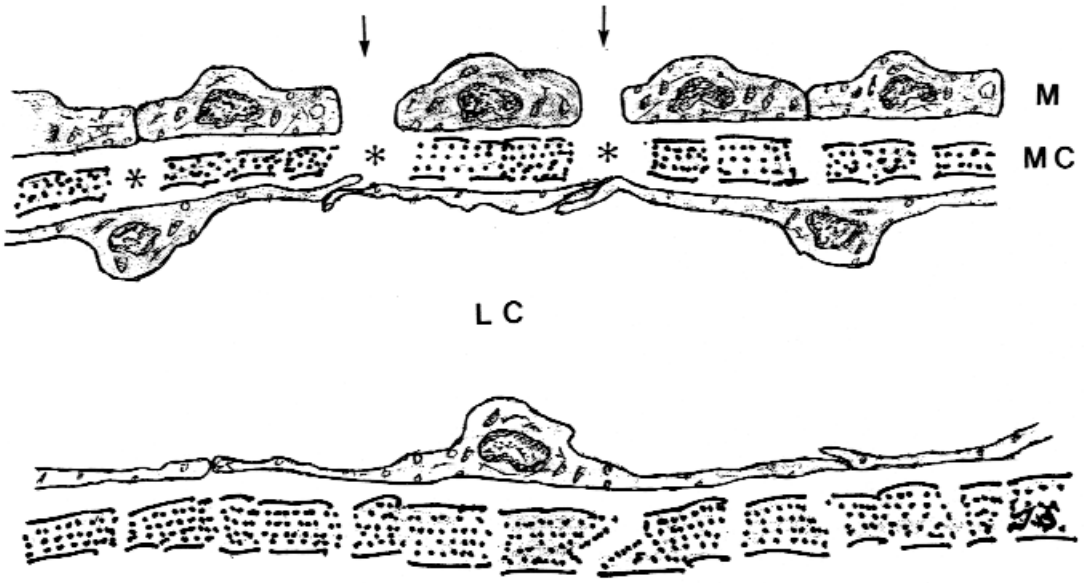

Fig 12. Diagram showing the lymphatic system in the parietal pleura. This system consists of mesothelial cells *(M)* with stomata *(arrows)*, macula cribriformis *(MC)* with foramina *(asterisks)*, and underlying lymphatic capillary (lacuna) *(LC)*.

stored in the foramina of the macula cribriformis; this strongly supports Kihara's thesis[9] that the macula cribriformis functions as a prelymphatic pathway. Masada's enzyme histochemical study[8] of the monkey parietal pleura illustrated that the diaphragmatic pleura had initial and collecting lymphatics. In our experiment, the intrapleurally injected carbon particles were still not visible within the lymphatics of the diaphragmatic pleura 1 hour after injection.

In contrast, video-assisted thoracoscopic observation demonstrated that the intrapleurally injected carbon particles drained to the diaphragmatic pleura as early as 10 minutes after injection. This finding may be due to the fact that the myogenic activity of the diaphragm greatly contributes to lymphatic drainage.[21-23] From our continuous observation by video-assisted thoracoscopy, we showed that intrapleurally injected carbon particles were absorbed throughout the costal, mediastinal, and diaphragmatic pleura and that the main route of drainage of the pleural cavity was the parasternal lymphatic system. According to the x-ray data of Pereira and Grande,[24] the translocation of tungsten powder ($CaWO_4$) from the pleural space to regional lymph nodes is a rapid process in the normally breathing dog and is first directed to the parasternal lymph nodes. Video-assisted thoracoscopy, which we used to investigate the lymphatic drainage of the parietal pleura of the monkey during normal breathing, also seems to be very useful for experimental study.

Recently, attention has been focused on intrapleural lavage cytology at thoracotomy in patients with no evidence of carcinomatous pleuritis, because the prognosis of patients with positive cytologic findings is poor compared with that of patients with negative findings.[25-29] Although the reason for this poor prognosis is not well understood, the lymphatic system of the parietal pleura may be one of the routes by which cancer cells in the pleural space migrate to systemic organs.

As shown in Fig 12, this system consists of mesothelial cells with stomata, the macula cribriformis, and underlying lymphatic lacunae, being similar to that in the diaphragmatic peritoneum.[14,15] The mesothelial stomata act as the entrances for cellular elements and macromolecules from the pleural cavity into the subpleural lymphatic lacunae. In our study, a great number of carbon particles were stored in the foramina of the macula cribriformis. Certainly, this finding may not be concisely adaptable to the pathway of tumor cells, because carbon particles, as shown in the figures, are too small as compared with tumor cells. Nevertheless, according to the previous studies in the diaphragmatic peritoneum, not only carbon particles but cellular elements such as macrophages,[14] erythrocytes,[15] and tumor cells[13] also could pass via the peritoneal stomata and the macula cribriformis into the lymphatic lacunae. Therefore, we suggest that the poor prognosis of patients with positive cytologic findings on pleural lavage might be due to the nature of the structure of the parietal pleura.

We thank Dr H. Kitamura, Mr S. Tatsukawa, Mr H. Kawasato, and Miss Goto for their technical support.

REFERENCES

1. Lemon WS, Higgins GM. Lymphatic absorption of particulate matter through the normal and paralyzed diaphragm: experimental study. Am J Med Sci 1929;178:536-47.
2. Courtice FC, Morris B. The effect of diaphragmatic movement on the absorption of protein and of red cells from the pleural cavity. Aust J Exp Biol Med Sci 1953;31:227-38.
3. Pinchon MC, Bernaudin JF, Bignon J. Pleural permeability in the rat. I. Ultrastructural basis. Biol Cell 1980;37:269-72.
4. Mariassy AT, Wheeldon EB. The pleura: a combined light microscopic, scanning and transmission electron microscopic study in the sheep. 1. Normal pleura. Exp Lung Res 1983;4:293-313.
5. Wang NS. The prefomed stomas connecting the pleural cavity and lymphatics in the parietal pleura. Am Rev Respir Dis 1975;111:12-20.
6. Kato S. Enzyme-histochemical method for identification of lymphatic capillaries. Lymphology 1991;24:125-9.
7. Kato S, Yasunaga A, Uchida Y, Fujiwara T. Enzyme-histochemical method to distinguish lymphatic capillaries from blood capillaries. Jpn J Lymph 1990;13:19-24.
8. Masada S, Ichikawa S, Nakamura Y, Uchino S, Kato H. Structure and distribution of the lymphatic vessels in the parietal pleura of the monkey as studied by enzyme-histochemistry and by light and electron microscopy. Arch Histol Cytol 1992;55:525-38.
9. Kihara T. Das extravaskulare Saftbahnsystem. Okajimas Fol Anat Jpn 1956;28:601-21.
10. Kihara T. Studies on the system of extra-vascular fluid pathway. Anat Rec 1960;136:318.
11. Tubouti M. Uber die siebformige Struktur des subendothehelialen Bindegewebes, Macula oder Membrane cribriformis, vorgefunden in der Pleura und im Peritonaeum der Wirbeltiere und des Menschen. Acta Anat Nippon 1950a;25:6-9.
12. Tubouti M. Die Entwicklung der Maculae cribriformes im menschlichen Bauch und Brustfell. Acta Anat Nippon 1950b;25:44-7.
13. Yamamoto M, Matsuoka S, Fukushima N, Kido M, Miyamoto T, Maeda K, et al. Cancer spread via extravascular fluid pathway. Arch Jpn Chir 1960;29:1456-73.
14. Oya M, Shimada T, Nakamura M, Uchida Y. Functional morphology of the lymphatic system in the monkey diaphragm. Arch Histol Cytol 1993;56:37-47.
15. Shimada T, Zhang L, Oya M. Architecture and function of the extravascular fluid pathway: special reference to the macula cribriformis in the diaphragm. Acta Anat Nippon 1995;70:140-55.
16. Hagiwara A. Mitomycin C absorbed to activated carbon particles as a new drug dosage form for cancer chemotherapy. Akita J Med 1983;10:187-229.
17. Huang CT, Iimura A. Stomata and lymphatic vessels in rat costal pleura. Lymphology 1992;15:1-11.
18. Nakatani T, Shinohara H, Fukuo Y, Morisawa S, Matsuda T. Pericardium of rodents: pores connect the pericardial and pleural cavities. Anat Rec 1988;220:132-7.
19. Wang QX, Ohtani O, Saitoh M, Ohtani Y. Distribution and ultrastructure of the stomata connecting the pleural cavity with lymphatics in the rat costal pleura. Acta Anat 1997;158:255-65.
20. Masada S, Nakamura Y, Nakamura H, Matsushima Y, Kawade N, Noguchi M, et al. Distribution and structure of lymphatics in the human diaphragmatic and mediastinal pleura. Jpn J Lung Cancer 1995;35:875-81.
21. Negrini D, Ballard ST, Benoit JN. Contribution of lymphatic myogenic activity and respiratory movements to pleural lymph flow. J Appl Physiol 1994;76:2267-74.
22. Negrini D, Massimo F, Canzio G, Silvano M, Giuseppe M. Distribution of diaphragmatic lymphatic lacunae. J Appl Physiol 1992;72:1166-72.
23. Broaddus VC, Wiener-Kronish JP, Berthiaume Y, Staub NC. Removal of pleural liquid and protein by lymphatics in awake sheep. J Appl Physiol 1988;64:384-90.
24. Pereira AS, Grande NR. Particle clearance from the canine pleural space into thoracic lymph nodes: an experimental study. Lymphology 1992;25:120-30.
25. Kondo H, Asamura H, Suemasu K, Goya T, Tsuchiya R, Naruke T, et al. Prognostic significance of pleural lavage cytology immediately after thoracotomy in patients with lung cancer. J Thorac Cardiovasc Surg 1993;106:1092-7.
26. Eagan RT, Bernatz PE, Payne WS, Pairolero PC, Williams DE, Goellner JR, et al. Pleura lavage after pulmonary resection for bronchogenic carcinoma. J Thorac Cardiovasc Surg 1984; 88:1000-3.
27. Buhr J, Berghauser KH, Morr H, Dobroschke J, Ebner HJ. Tumor cells in intraoperative pleural lavage: an indicator for the poor prognosis of bronchogenic carcinoma. Cancer 1990;65:1801-4.
28. Ichinose Y, Yano T, Aso H, Yokoyama H, Fukuyama Y, Katsuda Y. Diagnosis of visceral pleural invasion in resected lung cancer using a jet stream of saline solution. Ann Thorac Surg 1997;64:1626-9.
29. Kjellberg SI, Dresler CM, Goldberg M. Pleural cytologies in lung cancer without pleural effusions. Ann Thorac Surg 1997;64:941-4.